Current-fed Push-Pull type high frequency resonant inverter for wax-sealing

Jae-Sun Won*, Dong-Hee Kim*, Chae-Cyun Ro*, Min-Huei Kim**

School of Electrical and electronic Engineering, Yeungnam University*
214-1, Dae-Dong, Kyeungsan, Kyeungbuk, 712-749, South Korea
Yeungnam College of Science & Technology**
1737, Tae myeung-dong, Nan-gu, Taegu, 705-037, South Korea.

Abstract

This paper describes a double-ended current fed push-pull type high frequency resonant inverter used as the power supply for wax-sealing The proposed inverter can realize ZVS operation by using resonant capacitor to ZVS capacitor and has some merits not only reduction of switch current distribution but also extension of load range compare to the conventional single-ended current fed push-pull type high frequency resonant inverter. This analysis of proposed circuit uses normalized parameter and characteristic estimation which is needed in each step before design is generally described according to normalized frequency(μ), normalized resistance(λ) and parameters It is also presented as an example of method of the circuit design based on estimation analysis values from theoretical analysis. The theoretical analysis is proved through experiment and this circuit shows that it can be used practically as the power supply system for wax-sealing and DC-DC converter

1. Introduction

In recent years, according to using a power semiconductor device which has advantageous characteristics of high speed switching and small driving power, switching frequency of power conversion system has been ranging from tens of kHz to hundreds of kHz[1-3]. In driving a power switching semiconductor device to high speed switching, there are some problems such as dv/dt and di/dt stress, EMI problem, increase of switching loss due to charge dump of the switching device, the leakage inductance in the circuit. Thus, in order to remove them, this paper introduced soft switching techniques such as ZVS, ZCS, ZVZCS and E-class switching to reduce turn on and off loss at switching.[4] Also, this paper presents that a double-ended current-fed push-pull type high frequency resonant inverter can reduce current distribution of switch by connecting two inverter of the conventional single ended current fed push-pull type inverter parallel and resonant capacitor can be used as ZVS capacitor. The analysis of inverter circuit is generally described by using normalized parameter and operating characteristics have been evaluated by switching frequency and parameters.

A method of the circuit design is presented through the result of circuit analysis from theoretical analysis. In addition, this paper proves the validity of theoretical analysis through experiment in putting wax-sealing to induction heating load and applying power-MOSFET to switching devices of inverter circuit.

2. Characteristics analysis

2.1. Principle of induction-heating for wax-sealing

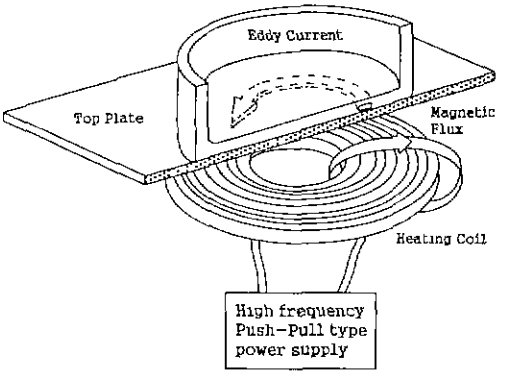

Fig.1. Principle of induction-heating for wax-sealing

Power supply for wax-sealing is a high frequency oscillating power system, to preserve something in plastic box longer, for sealing up thin aluminum plate. Wax-sealing power system needs small size and light weight because it needs heating up not whole part of thin aluminum plate but only sealed side for a short time. Accordingly, high frequency induction heating is appropriate for sealing efficiency in heating sealed part with skin effect. In induction heating,

when high frequency current flows in all conductor including cylindrical conductor, the deeper the position from surface to center, the less the current density. Most heating energy is within the skin depth(δ) in Eq. (1), that is if the skin depth(δ) is made be thin by high frequency, the surface part of only needed depth has intense heat.

$$\delta = \sqrt{\frac{1}{4\pi \times 10^{-7}}} \sqrt{\frac{\rho}{\mu f}} \qquad (1)$$

where, ρ. electrical resistivity of work-piece ($\Omega \cdot$m)

μ : magnetic permeability

f: applied frequency (Hz)

The basic concepts are similar to transformer theory, but modified to a single turn short-circuited secondary winding. the induction heating load (heating coil and work-piece) can be modified by means of a series combination of its equivalent resistance(R) and inductance(L).[5]

2.2. Circuit configuration

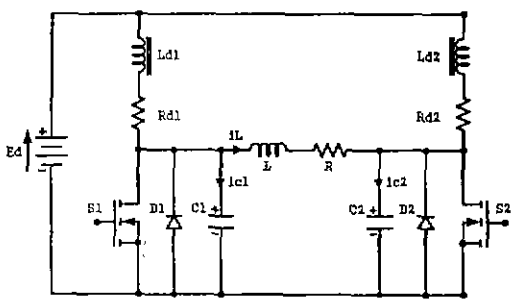

Fig. 2 A double-ended current fed push-pull type high frequency resonant inverter.

Fig. 2. shows a double-ended current fed push-pull type high frequency resonant inverter proposed in this paper. The circuit scheme, as shown in Fig 2, is composed of the resonant inverter which reduces turn on and off loss generating in the switching devices at switching using inactive devices with ZVS function as resonant capacitors(C1, C2). The resonant capacitors(C1, C2) are connected in parallel with the switches(S1, S2).

The reactors(Ld1, Ld2) are to provide constant current which has small ripple from Ed and the switching devices(S1, S2) can be used in all switching device with self-turn off function and diodes(D1, D2) is used to by pass ineffective current flowing in the circuit that has been shown in the circuit operating characteristics. The induction heating load is employed to wax-sealing and the resonant circuit configuration in Fig. 2 consists of working-coil(R-L), parallel resonant capacitor (C1, C2) and switching devices(S1, S2), diodes(D1, D2) respectively. The circuit configuration shows that the proposed inverter has following strengthen points. First point is that configuration of circuit is easy. Second point is that this current fed inverter can be operated ZVS operation. Next point is that resonant capacitor is used as ZVS capacitor.

Last point is that it has smaller switch current distribution than in the conventional single-ended current-fed push-pull type inverter and also has advantage that the region of load is eminently extended compare to its inverter.

2.3. Circuit analysis

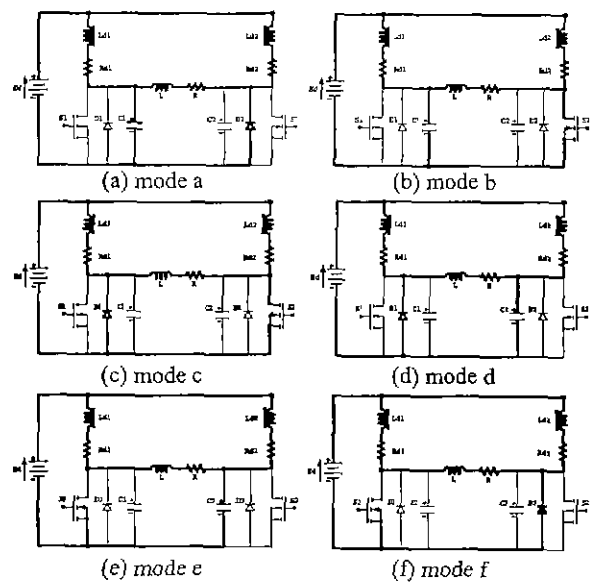

Fig 3. Switching operation mode

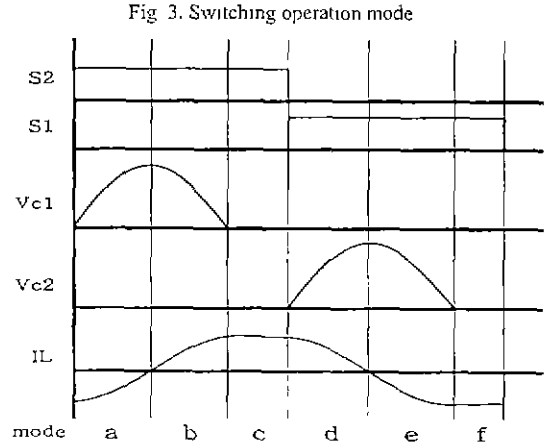

Fig 4. Wave forms of resonant capacitors(C1, C2) voltage and load current by gate pulse

The switching operation mode of the proposed inverter is classified into six modes by on/off operation of switches(S1, S2), diodes(D1, D2) and the charge and discharge of resonant capacitor (C1, C2) across switches(S1, S2). Fig. 3 shows each of switching operating mode and Fig 4 shows wave forms of resonant capacitor(C1, C2) voltage and load current by gate pulse. In order to generalize of circuit analysis to the state equation of each mode, the circuit state equation is introduced to normalized parameter which shown in Table 1.

Table 1. Normalized parameters

	Reference Values	Normalized Values
Voltage	E_d	$v^*(z)=v(t)/E_d$
Current	$I=E_d/Z_s$	$i^*(z)=i(t)/I$
Time	$T_{sw}=1/f_{sw}$	$z=t/T_{sw}$
Frequency	$f_r=1/2\pi\sqrt{L_s C_s}$	$\mu=f_{sw}/f_r$
Impedance	$Z_S=2\sqrt{L_s/C_s}$	$\lambda=R/Z_S$
Power	$P_s=E_d \cdot I_s$	$P^*(z)=P(t)/P_s$

<Remarks>
f_{sw} : Operating Frequency of Inverter
T_o : Operating Period of Inverter
$L_s=L$, $C_s=C_1=C_2$, $i_d{}^*=i_{d1}{}^*=i_{d2}{}^*$
$a=L_{d1}/L=L_{d2}/L$

The normalized circuit state equation of each switching mode in Fig 3 are described as follows

$$\frac{dX^*}{dz^*}=A^* \cdot X^* + B^* \cdot U^* \qquad Y^*=C \cdot X^* \qquad (2)$$

Where, $X^*=[i_{d1}{}^*(z),\ i_{d2}{}^*(z),\ i_L{}^*(z),\ v_{c1}{}^*(z),\ v_{c2}{}^*(z)]$
U=[0 0 1 0 0], A*, B*, C of each mode is as follows.

The marks concerning A*, B*, C of each mode is as follows.

$$E=-\frac{4\pi\lambda}{a\mu},\ F=\frac{8\pi}{a\mu},\ G=-\frac{4\pi(\lambda+\lambda_1)}{\mu(a+1)},\ H=-\frac{4\pi\lambda_1}{a\mu},$$

$$J=\frac{8\pi}{\mu(a+1)},\ K=-\frac{4\pi\lambda}{\mu},\ L=\frac{4\pi}{\mu},\ M=\frac{\pi}{2\mu},\ N=\frac{\pi}{\mu}$$

MODE a

$$A^*=\begin{bmatrix} E & 0 & 0 & -F & 0 \\ 0 & G & 0 & -J & 0 \\ 0 & 0 & K & L & 0 \\ M & 0 & -N & 0 & 0 \\ 0 & 0 & 0 & 0 & 0 \end{bmatrix}$$

$B^*=[\,F \quad J \quad 0 \quad 0 \quad 0\,]^T$

$C=[\,0 \quad 0 \quad 1 \quad 0 \quad 0\,]$ (3)

MODE b

$$A^*=\begin{bmatrix} E & 0 & 0 & -F & 0 \\ 0 & H & 0 & 0 & 0 \\ 0 & 0 & K & L & 0 \\ M & 0 & -N & 0 & 0 \\ 0 & 0 & 0 & 0 & 0 \end{bmatrix}$$

$B^*=[\,F \quad F \quad 0 \quad 0 \quad 0\,]^T$

$C=[\,0 \quad 0 \quad 1 \quad 0 \quad 0\,]$ (4)

MODE c

$$A^*=\begin{bmatrix} G & 0 & 0 & 0 & 0 \\ 0 & H & 0 & 0 & 0 \\ 0 & 0 & K & L & 0 \\ 0 & 0 & 0 & 0 & 0 \\ 0 & 0 & 0 & 0 & 0 \end{bmatrix}$$

$B^*=[\,J \quad F \quad 0 \quad 0 \quad 0\,]^T$

$C=[\,0 \quad 0 \quad 1 \quad 0 \quad 0\,]$ (5)

MODE d

$$A^*=\begin{bmatrix} G & 0 & 0 & 0 & -J \\ 0 & H & 0 & 0 & -F \\ 0 & 0 & K & 0 & -L \\ 0 & 0 & 0 & 0 & 0 \\ 0 & M & N & 0 & 0 \end{bmatrix}$$

$B^*=[\,J \quad F \quad 0 \quad 0 \quad 0\,]^T$

$C=[\,0 \quad 0 \quad 1 \quad 0 \quad 0\,]$ (6)

MODE e

$$A^*=\begin{bmatrix} H & 0 & 0 & 0 & 0 \\ 0 & H & 0 & 0 & -F \\ 0 & 0 & K & 0 & -L \\ 0 & 0 & 0 & 0 & 0 \\ 0 & M & N & 0 & 0 \end{bmatrix}$$

$B^*=[\,F \quad F \quad 0 \quad 0 \quad 0\,]^T$

$C=[\,0 \quad 0 \quad 1 \quad 0 \quad 0\,]$ (7)

MODE f

$$A^*=\begin{bmatrix} H & 0 & 0 & 0 & 0 \\ 0 & G & 0 & 0 & 0 \\ 0 & 0 & K & 0 & 0 \\ 0 & 0 & 0 & 0 & 0 \\ 0 & 0 & 0 & 0 & 0 \end{bmatrix}$$

$B^*=[\,F \quad J \quad 0 \quad 0 \quad 0\,]^T$

$C=[\,0 \quad 0 \quad 1 \quad 0 \quad 0\,]$ (8)

3. Characteristic estimation

In order to examine that DC input reactors(Ld1, Ld2) influences on circuit operation, Figure 5(a) and Figure 5(b) shows the ripple characteristics($Id1^*rip$) of DC input reactor current according to the variation of (α, μ) with λ=0.03 and the variation of (α, λ) with μ=1.0 respectively The ripple factor of DC input reactor is defined as follows.

$$RF=\frac{V_{ac}}{V_{dc}}=\sqrt{\frac{V^2_{rms}-V^2_{dc}}{V^2_{dc}}}\times 100\ [\%] \qquad (9)$$

Fig 5 shows that when α is more than 10, the ripple ratio is somewhat decreased and as μ is decreased or λ is increased, in the case of a fixed α, the ripple ratio is increased.

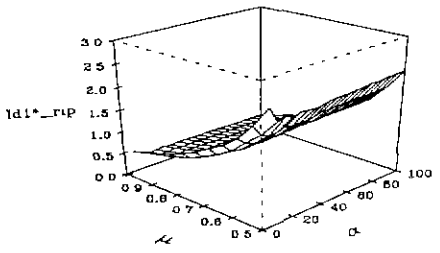

(a)

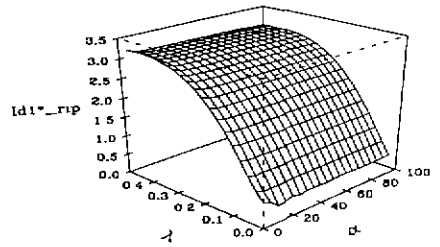

(b)

Fig. 5. The ripple characteristics of the DC input reactor

Accordingly, when DC input reactors(Ld1, Ld2) are over ten times as much as resonant reactor, it is appropriate to consider voltage source circuit to current source circuit.

Fig. 6 shows the gain characteristics(*Gain**) of load current(i_L*) of DC input current(id*) in the proposed inverter according to the variation of (μ, λ) with α=100.

The current gain is defined as follows.

$$Current\ Gain^{*} = 20\log\frac{i_L^{*}}{i_d^{*}} \qquad (10)$$

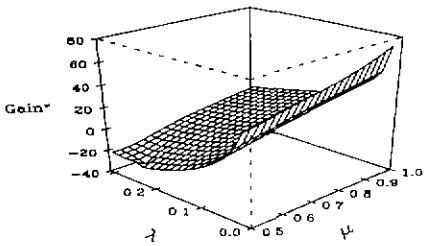

Fig. 6. gain characteristics of the current

Fig. 6 shows that when μ is about 1.0, the largest current gain characteristic is shown and when μ is far from 1.0, the current gain is decreased. Accordingly, when μ is about 1.0, the largest power is delivered from source to load because of impedance matching. As λ is increased, at fixed μ, the current gain is decreased and the current gain is lesser than zero with λ>0.1. Also, since the increase of λ brug about the increase of damping coefficient of load, the current gain have negative value because the DC input current(id_1*, id_2*) is larger than the load current.

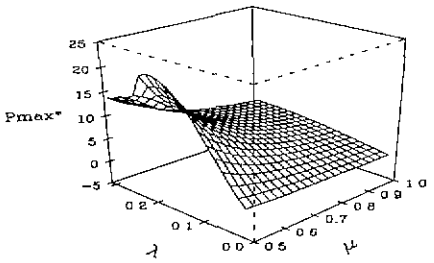

Fig. 7. Characteristics of the output power

Fig. 7 shows the output power characteristics (P_{max}*) according to the variation of (μ, λ) with α=100. As shown in Fig. 7, as μ is increased, at fixed λ, the output power is decreased. According to the variation of μ, the output power is the least when μ is about 1.0 and output power becomes bigger as μ is farther from 1.0. It is said that as the μ is far from the largest efficiency resonant point(μ=1.0), the inefficient power in load becomes bigger, which makes the load impedance small. As the result of this process, input current from source is increased, which makes (P_{max}*) be increased. Thus, the output power is the least when μ is about 1.0, but output power with high efficiency can be obtained because load includes not inefficient power but only efficient power

Fig 8 shows the peak characteristics of the switching current(I_{swmax}*) according to the variation of (μ, λ) with α=100. As λ is increased, the peak value of the switching circuit is decreased

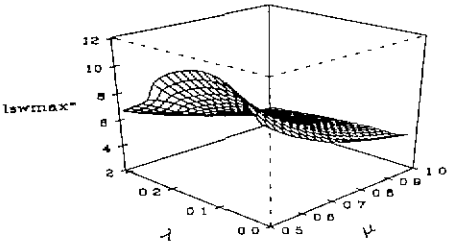

Fig. 8. Characteristics of the peak switch current

Fig 9 shows the characteristics of the peak capacitor voltage(V_{clmax}*) according to the variation of (μ, λ) with

α=100. As μ is increased, the peak value of the resonant capacitor is decreased. The peak voltage of the resonant capacitor is decided by the integrated value of current flowing through the switching device. The characteristic values of Fig 8 and Fig 9 are used as the important data which decides the resisting current of the switching device and the resisting voltage of resonant capacitor in the course of design.

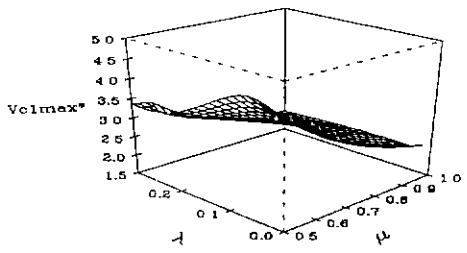

Fig. 9. Characteristics of the peak capacitor voltage

Fig.10 shows characteristic of voltage across switches according to the variation of μ with α=100 and λ= 0.03. As μ is increased, the slope of charge and discharge of resonant capacitor is smoothed. It is considered that the voltage distribution of voltage across switches is decreased with the increase of μ because the average voltage value across resonant capacitor become to nearly constant value during switching time of μ[1.0.

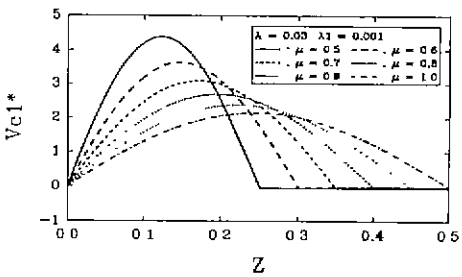

Fig. 10. Characteristics of the voltage across *vc1* * by μ

4. Circuit design and experiment

Based on the characteristic values obtained by the characteristic estimation through the circuit analysis, the design specification of the input voltage Ed(V), the output power P(kW) and the switching frequency fsw(kHz) are established. A method of the circuit design and operating characteristics of the inverter is as follows

Step 1 Decision of (μ, λ, P_{max}*) · Reference to Fig 7

Step 2 Calculation of basic impedance

$$P^*(z) = \frac{P(t)}{P_S} = \frac{P(t)}{E_d^{\,2}/Z_S}$$

$$Z_b = \frac{E_d^{\,2}\ P^*(z)}{P(t)} = 2\sqrt{\frac{L_S}{C_S}}$$

Step 3 Calculation of the circuit inherent frequency *fr(kHz)*

$$f_r = \frac{f_{sw}}{\mu} = \frac{1}{2\pi\sqrt{L_S C_S}}$$

Step 4 Calculation of *Ls, Cs, L_{d1}, L_{d2}*

Step 5 Calculation of the switch current and capacitor voltage

i_{swmax}* : Reference to Fig 8

v_{c1max}* : Reference to Fig 9

< The example of the circuit design>

Specification : *Ed=50(v), P=1(kW), fsw=470*(kHz)

Step 1 In the characteristic curves of Fig 7

Decision to μ =1.0, λ =0.03, P_{max}*=0.5441

Step 2 $Z_S = \frac{50^{\,2} \cdot 0.54441}{1000} = 1.36$

Step 3 $f_r = \frac{470}{1.0} = 470\ ,\ \sqrt{L_S C_S} = 338\ .6 \times 10^{-9}$

Step 4 From Step 2 and Step 3

Ls=4.74(μ H), *Cs=C_1=C_2=24.2*(nF)

L_{d1}=L_{d2}=334(μH)

Step 5 i_{swmax}* : 11.14A

v_{c1max}*, v_{c2max}* : 158.07V

In the case of exercising simulation through the numerical analysis using the Runge-Kutta with the design values as mentioned above, under the steady state of the proposed inverter, Fig. 11(a), (b) respectively shows the Pspice and theoretical wave forms of the load current(i_L) and the voltage across the switch(V_{c1},V_{c2}).

Fig. 12 shows the experimental wave forms of the load current(i_L) and the voltage across the switch(V_{c1}, V_{c2}) through the experimental test in order to prove the validity of the theoretical analysis. As shown in Fig. 11(a), (b) and Fig.12 the result of the theoretical, Pspice and experimental wave forms are in a good agreement. Table 2. shows the circuit parameters used in experiment.

Table 2. Experimental parameters

Circuit Parameter	Rating	Circuit Parameter	Rating
Input Voltage	50(V)	Load Resistor	0.5(Ω)
Power-MOSFET (IRFP 360)	400(V) 28(A)	Resonant Reactor(L)	4.74(μH)
Input Reactor (Ld1, Ld2)	334(uH)	Resonant Frequency	470(kHz)
Resonant Capacitor (C1, C2)	24 2(nF) 640(V)	ıLmax	11.14(A)
		Vc1max, Vc2max	158.07(V)

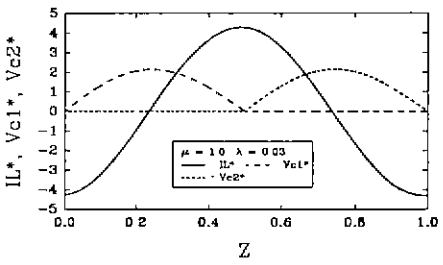

(a)

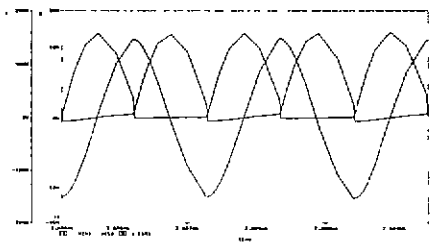

(b)

Fig. 11 Theoretical and Pspice wave forms

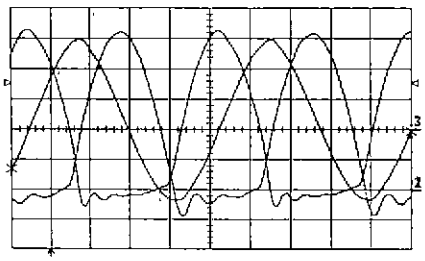

(Voltage(Vc1, Vc2) : 30(V)/dıv, Current : 4((A)/dıv)

Fig. 12 Experimental wave forms

5. Conclusion

Thus paper presents a double-ended current fed push-pull type high frequency resonant inverter, which can be used resonant capacitor as ZVS capacitor and made the conventional single-ended current fed push-pull type high frequency resonant inverters parallel.

The followings are obtained from this study

1. Current distribution of switch is decreased and the region of load is extended compared to the conventional single-ended current fed push-pull type high frequency resonant inverter.
2. Characteristic estimation, which is needed in the step before design, is described through normalized parameter in considering wax-sealing as the induction heating load in the proposed inverter..
3. An example of method of the circuit design from theoretical analysis is proposed and experimental wave forms tends to be similar to theoretical wave forms through experiment using power-MOSFET as switching device.

   This propose inverter shows that it can be practically used as power source system for wax-sealing and DC-DC converter etc.

References

[1] W. E. Frank et. al: ``New Induction Heating Transformers'', IEEE, Vol. MAG18, NO. 6, pp. 1752-1755, 1982

[2] Guan-C yun Hsieh, Chun-Hung Lin, Jyh-Ming Li and Yu-Chang Hsu, ``A study of series-resonant DC/AC Inverter'', in Proceedings of the 1995 IEEE Pesc95, Vol. 1. pp. 493-499.

[3] A. Takeuchi et al : ``Zero-Voltage-Switching Controlled High Power-Factor Converter'', PESC'96, Vol. 1. pp. 1859-1864, 1996.

[4] S.P.Wang, M Nakaoka, K.Izaki, I.Hirota, H.Yamashida and H.Omori, ``Soft-Switched PWM High-Frequency Load-Resonant with Power Factor Correction for Induction Heating Cooking Appliance, EPE'97 Vol. 2. pp. 244-249.

[5] Mokhtar Kamli, Shigehiro Yamamoto, and Minoru Abe, ``A 50-150 kHz Half-Bridge Inverter for Induction Heating Applications'', IEEE Trans on Industrial Electronics, Vol. 43, No. 1, FEB, pp. 163-172 1996

[6] Jong-Hae Kim, Dong-Hee Kim and Chae-Gyan Ro etc, ``A study on the ZVS-SEPP type high frequency resonant inverter with induction heating jar(l) '', Trans. KIEE Vol. 48B, No 2, pp 69-74, FEB 1999